# JCI insight

# Mass cytometry identifies distinct CD4⁺ T cell clusters distinguishing HIV-1–infected patients according to antiretroviral therapy initiation

Yonas Bekele, … , Petter Brodin, Francesca Chiodi

Research Article    AIDS/HIV    Immunology

Recent guidelines recommend antiretroviral therapy (ART) to be administered as early as possible during HIV-1 infection. Few studies addressed the immunological benefit of commencing ART during the acute phase of infection. We used mass cytometry to characterize blood CD4⁺ T cells from HIV-1–infected patients who initiated ART during acute or chronic phase of infection. Using this method, we analyzed a large number of markers on millions of individual immune cells. The results revealed that CD4⁺ T cell clusters with high expression of CD27, CD28, CD127, and CD44, whose function involves T cell migration to inflamed tissues and survival, are more abundant in healthy controls and patients initiating ART during the acute phase; on the contrary, CD4⁺ T cell clusters in patients initiating ART during the chronic phase had reduced expression of these markers. The results are suggestive of a better preserved immune function in HIV-1–infected patients initiating ART during acute infection.

## Find the latest version:

JCI insight

# Mass cytometry identifies distinct CD4+ T cell clusters distinguishing HIV-1–infected patients according to antiretroviral therapy initiation

Yonas Bekele,[1] Tadepally Lakshmikanth,[2] Yang Chen,[2] Jaromir Mikes,[2] Aikaterini Nasi,[1] Stefan Petkov,[1] Bo Hejdeman,[3] Petter Brodin,[2,4] and Francesca Chiodi[1]

[1]Department of Microbiology, Tumor and Cell Biology, Biomedicum, and [2]Science for Life Laboratory, Division of Clinical Pediatrics, Department of Women's and Children's Health, Karolinska Institutet, Stockholm, Sweden. [3]Department of Clinical Science and Education, Södersjukhuset, Karolinska Institutet, and Unit of Infectious Diseases, Venhälsan, Södersjukhuset, Stockholm, Sweden. [4]Department of Newborn Medicine, Karolinska University Hospital, Stockholm, Sweden.

**Recent guidelines recommend antiretroviral therapy (ART) to be administered as early as possible during HIV-1 infection. Few studies addressed the immunological benefit of commencing ART during the acute phase of infection. We used mass cytometry to characterize blood CD4+ T cells from HIV-1–infected patients who initiated ART during acute or chronic phase of infection. Using this method, we analyzed a large number of markers on millions of individual immune cells. The results revealed that CD4+ T cell clusters with high expression of CD27, CD28, CD127, and CD44, whose function involves T cell migration to inflamed tissues and survival, are more abundant in healthy controls and patients initiating ART during the acute phase; on the contrary, CD4+ T cell clusters in patients initiating ART during the chronic phase had reduced expression of these markers. The results are suggestive of a better preserved immune function in HIV-1–infected patients initiating ART during acute infection.**

## Introduction

Introduction of antiretroviral therapy (ART) has substantially improved quality of life and life expectancy for HIV-1–infected patients. WHO guidelines from 2015 proposed ART to be started in all HIV-1–infected adults during the acute phase of HIV-1 infection, with the aim of preventing immunological decline in infected patients and HIV-1 driven inflammation; early ART initiation may also have a substantial impact on the HIV-1 epidemic by decreasing the risk of HIV-1 transmission between individuals. An important drive to the revised WHO recommendations mentioned above was a study showing that initiation of ART during the early asymptomatic stage of infection led to a clear clinical benefit compared with ART administration during the chronic phase of infection (1); the clinical benefit was quantified through a cumulative clinical primary endpoint, which gathered serious AIDS-related events with non–AIDS-related events. The delayed outcome of a primary endpoint was also observed following short-course ART during primary HIV-1 infection, measured as CD4+ T cell count of less than 350 cells/μl or subsequent long-term ART initiation (2).

In spite of prolonged ART intervention, HIV-1 establishes cellular latency in treated patients, mostly in resting memory T cells, which make up the cellular HIV-1 reservoirs (3). Studies are still ongoing to assess the beneficial effect of ART initiated during acute HIV-1 infection on the size of virus reservoirs. Initiation of ART early during acute infection led to the formation of smaller size HIV-1 reservoirs (4), compared with reservoirs formed in patients initiating ART during the chronic phase of infection. The reduced size of HIV-1 DNA reservoirs promoted by early ART initiation was sustained following 3 years of therapy (5). At 24 months from ART initiation, we found a significantly lower number of HIV-1 DNA copies in PBMCs of patients who initiated ART during the acute phase of infection, compared with patients who initiated ART during the chronic phase of infection (6).

Phenotypic and functional dysfunctions that affect CD4^{+} and CD8^{+} T cells during HIV-1 infection are only partially corrected by ART initiated during the chronic phase of infection. An extensive number of studies conducted with flow cytometry revealed the abnormal expression of immune activation and senescence markers in ART-treated patients. Very few studies, however, have addressed whether ART initiation during the early phase of HIV-1 infection prevents the establishment of phenotypic and functional abnormalities of CD4^{+} and CD8^{+} T cells. The gastrointestinal (GI) tract is an important compartment to study in this context because HIV-1 replication in this organ system causes a massive loss of CD4^{+} T cells (7), followed by fenestration of the epithelial barrier and microbial translocation. Deleage and collaborators (8), using in situ IHC methods, recently addressed the questions of whether GI tract pathologies, including loss of CD4^{+} T cells, inflammation, and immune activation, are established during acute HIV-1 infection in humans and whether they are prevented and controlled by early ART administration. Their study (8) clearly demonstrated that immune dysfunctions in the GI tract are established very early during acute infection and are not preventable by ART initiated during acute infection; in addition, immunological damage can also take place in the GI tract following a period of several months of ART initiated during acute infection. The results from a study recently published by our group (6) showed that an equivalent abnormal expression of activation and terminal differentiation markers was found in blood T cells of patients initiating treatment during the acute and chronic phase of HIV-1 infection and maintained on continuous ART treatment for 24 months. The findings from the above studies are worrisome because they suggest that abnormalities established in the T cell compartment during acute HIV-1 infection are not corrected by early ART initiation.

More sensitive methods should be applied to study the relation between immunological abnormalities and time of ART initiation during HIV-1 infection. Mass cytometry offers the possibility of analyzing up to 45 parameters measured simultaneously at the single-cell level. Studies of T cell subsets with mass cytometry in healthy and diseased individuals provide an opportunity to evaluate the heterogeneity and coregulation of immune cell populations across the entire blood immune system (9–13). To establish whether initiation of ART during acute infection leads to a measurable immunological benefit compared with ART initiation during the chronic phase of infection is of pivotal relevance. Here, by using mass cytometry, we studied CD4^{+} T cell subsets from peripheral blood of HIV-1–infected patients treated with ART at the early (acute; EA) and late (chronic; LA) phases of infection and compared these with blood samples obtained from healthy controls. The Citrus algorithm was used to identify differentially regulated cell populations (14), and the t-distributed stochastic neighbor embedding (t-SNE) algorithm (15, 16) was used for visualization of T cell populations at single-cell resolution. Mass cytometry analyses identified clusters of T cells, discriminating HIV-1–infected patients treated early and late as well as healthy controls. These findings suggest that changes involving the markers CD44, CD27, CD28, and CD127 represent a signature of functional CD4^{+} T cell decline in patients treated during chronic as compared with acute HIV-1 infection.

## Results

*Clinical parameters of individuals starting ART during the acute and chronic phases of HIV-1 infection.* The clinical characteristics of healthy controls (HCs) and HIV-1–infected individuals included in the study are shown in Table 1. Before ART initiation, the EA group had significantly higher (*P* = 0.03) HIV-1 RNA copies (median 5.79 log/ml) compared with the LA group (4.80 log RNA copies/ml). HIV-1 RNA copies were reduced to levels below the detection limit (<20 copies/ml) in all HIV-1–infected subjects at the time of sampling (Table 1). The CD4^{+}/CD8^{+} T cell ratio was significantly higher in EA compared with LA study participants both at 12 months after ART initiation (median 1.35 versus 0.76, *P* < 0.001) and during sampling conducted at approximately 24 months from ART initiation (median 1.37 versus 0.81, *P* < 0.0001). The size of the HIV-1 reservoirs was measured (6), and the LA group had a significantly higher number of total HIV-1 DNA copies in PBMCs compared with the EA group at the time of sampling (*P* = 0.03).

*Immunostainings of T cell subpopulations.* The frequencies of naive, central memory (CM), and effector memory (EM) CD4^{+} T cell subpopulations were determined in HCs and HIV-1–infected patients (Figure 1). The frequencies of these subpopulations did not differ significantly between the 3 groups. The mean frequency value of naive CD4^{+} T cells was 27.6% (SD ± 14.3) for controls, 30.1% (± 9.9) for EA, and 32.8% (± 10.0) for LA patients; for CM CD4^{+} T cells it was 43.5% (SD ± 11.4) for controls, 36.5% (± 4.5) for EA patients, and 39.1% (± 11) for LA patients. The mean frequency values of EM CD4^{+} T cells were 26.9% (SD ± 9.2) in controls, 31.2% (± 12.8) for EA, and 24.6% (± 6.3) for LA.

**Table 1. Clinical characteristics of HIV-1–infected individuals and HCs[A]**

| Characteristics | HCs ($n = 10$) | EA ($n = 10$) | LA ($n = 10$) | P values |
|---|---|---|---|---|
| Age (years) | 38.5 (26–64) | 41 (27–66) | 41 (29–62) | NS |
| Length of ART treatment (months) | NA | 23 (7–59) | 31.5 (13–46) | NS |
| Before ART | | | | |
| RNA copies/ml (log) | NA | 5.79 (3.17–7) | 4.8 (3.57–6.63) | 0.03 |
| At sampling | | | | |
| RNA copies/ml | NA | <20 | <20 | NS |
| CD4+ T cell counts | NA | 1,010 (450–1,340) | 795 (610–1,000) | NS |
| CD4+/CD8+ ratio | NA | 1.37 (1.08–1.58) | 0.81 (0.69–1.01) | <0.0001 |
| HIV-1 DNA copies/10^6 PBMCs | NA | 380 (80–3,669) | 1,985 (10–20,029) | 0.03 |

[A]All values, except RNA copies/ml, are median values with range.

*Distinct clusters distinguish CD4+ T cells of HCs from HIV-1–infected individuals.* Two sets of analyses were conducted to evaluate cluster differences between HCs and HIV-1–infected individuals and between the EA and LA HIV-1–infected groups.

Within the CD4+ T cell population, the Citrus algorithm identified 19 individual CD4+ T cell clusters that significantly differed in abundance between HCs, EA individuals, and LA individuals. Among the 19 clusters, 12 were more abundant in HCs as compared with HIV-1–infected patients (HCs>EA>LA) (Figure 2A). Five clusters were more abundant in LA patients with compared to HCs and EA patients (LA>HCs>EA) (Figure 2B). In addition, 2 clusters were more abundant in LA patients compared with EA patients and HCs (LA>EA>HCs) (Figure 2C). The hierarchical clustering by Citrus showed that these 19 clusters represent 2 distinct groups of cells (Figure 3); the 12 clusters included in group 1 were dominated by cells from HCs, while the 7 clusters in group 2 were dominated by cells from LA patients.

A heatmap was then created to visualize differences in marker expression across the substantially different CD4+ T cell clusters (Figure 4, A and B, and Tables 2 and 3). Based on the difference in the levels of CD27, CD28, and CD127 expression, 2 main groups, overlapping the clusters included in groups 1 and 2 of Citrus networking visualizing hierarchical clusters of CD4+ T cells (Figure 3), were identified. Clusters with higher expression of CD27, CD28, and CD127 (corresponding to group 1 in Figure 3) were more abundant in HCs. These T cell populations also displayed a high and consistent expression of CD44. CD44 had originally been described as an adhesion molecule binding to hyaluronic acid (HA) and additional ligands and has gained attention recently as an activation marker distinguishing memory and effector T cells from their naive counterparts (17). The low expression of CD45RA in these 12 clusters, accompanied by high expression of CD27, CD28, CD127, and CD44, indicate that these clusters largely represent memory T cells. The 12 clusters included in group 1 could be further classified according to the expression of chemokine receptors CCR4 and CXCR3: A high expression of the T cell–trafficking molecule CXCR3 directing T cells to inflamed tissue was found in 5 clusters (clusters 449960, 449976, 449989, 449991, 449982); 3 clusters (clusters 449956, 449971, and 449980) showed a high expression of the chemokine receptor CCR4, a Th2-associated molecule. Finally, 4 clusters (clusters 449992, 449994, 449995, and 449997) expressed a moderate level of both chemokine receptors CCR4 and CXCR3. A consistent expression of the molecules HLA-DR and CD5 also characterized the clusters abundant in HCs.

Seven clusters were more abundant in LA patients compared with HCs and EA patients (Figure 4A). These clusters, corresponding to group 2 (Figure 3 and Tables 2 and 3), showed a consistently lower expression of CD28, CD27, CD127, and CD44 compared with the clusters more abundant in HCs; these phenotypical properties suggest the clusters consist of CD4+ T cells with an effector and terminally differentiated phenotype (EM and TEMRA), an observation supported from the higher CD45RA expression. On average, the expression of the chemokine receptors CCR4 and CXCR3 was reduced in group 2 clusters compared with group 1 (Figure 4B and Tables 2 and 3). Clusters 449978 and 449993 expressed substantial levels of CD57, a marker of senescent cells (Figure 4 and refs. 18, 19).

*The expression of CD44, CD27, CD28, and CD127 distinguishes CD4+ T cell clusters from EA and LA patients.* To determine whether ART initiation during acute HIV-1 infection would lead to a preserved CD4+ T cell phenotype, as compared with patients initiating ART during the chronic phase of infection, we compared CD4+ T cell populations from EA and LA groups of patients.
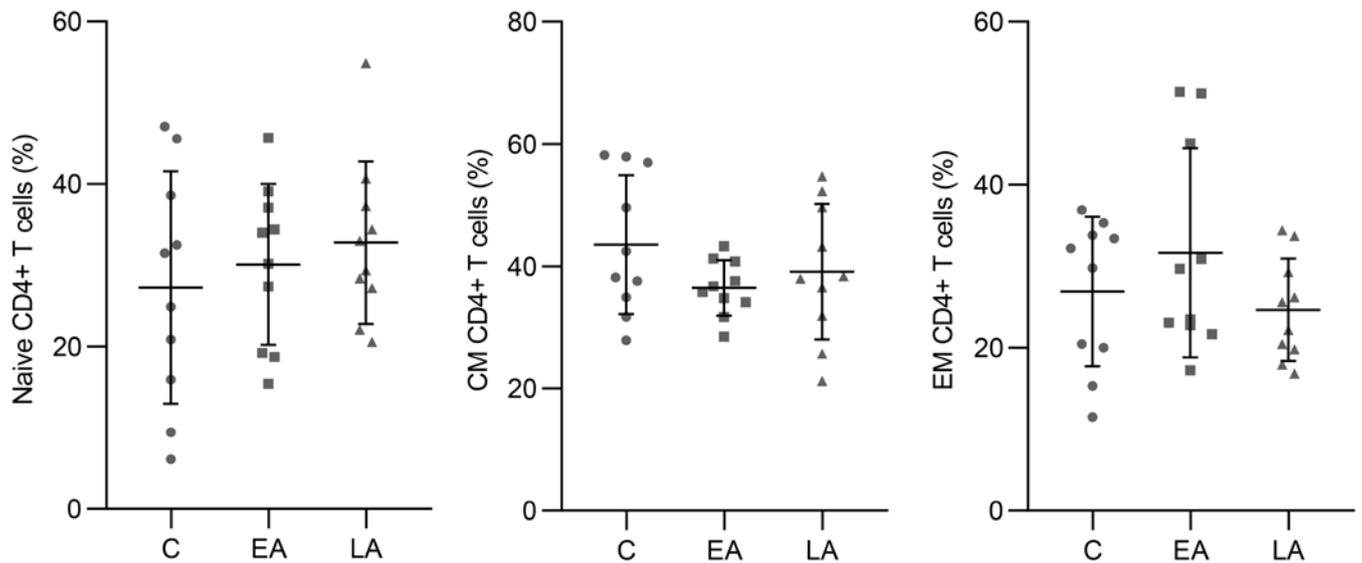
**Figure 1. Frequencies of CD4+ T cell subpopulations in HCs and EA and LA HIV-1–infected patients.** The frequencies (mean and SD) of naive, CM, and EM CD4+ T cells from HCs (*n* = 10), EA (*n* = 10), and LA (*n* = 10) are shown. ANOVA was used to assess differences between groups. This experiment was conducted 1 time. C: control. Symbols represent individuals; horizontal bars indicate the mean ± SD.

The analysis of the CD4+ T cells from EA and LA HIV-1 patients revealed 17 clusters that distinguished these 2 groups of patients; 10 clusters were more abundant in EA compared with LA individuals (Figure 5A), whereas 7 clusters were more abundant in LA individuals (Figure 5B). Citrus networking analysis showed a high cluster diversity between CD4+ T cells of EA and LA HIV-1–infected individuals; these clusters could be grouped into 2 major groups, defined as groups 3 and 4, and 4 distinct nodes, which were not further evaluated (Figure 6).

A heatmap was created showing the expression of markers in clusters included in groups 3 and 4 (Figure 7A), and the average expression of the markers is shown to evaluate differences between the 2 groups (Figure 7B and Tables 2 and 3). The expression of CD27, CD28, CD127, and CD44 was higher in clusters that were more abundant in EA patients. These EA clusters also showed a moderately higher expression of HLA-DR and CD5, CCR4, CXCR3, and CXCR5 compared with clusters that were more abundant in LA patients (Figure 7, A and B, and Tables 2 and 3). Interestingly, the clusters that were more abundant in LA patients, in addition to showing a lower expression of CD27, CD28, CD127, and CD44 markers, showed an increased expression of CD45RA and CD38 suggesting that the pressure leading to CD4+ T cell differentiation toward an effector phenotype with exhaustion characteristics is not reverted by ART initiated in the chronic phase of infection.

The phenotypic differences of clusters from EA and LA patients are also illustrated by t-SNE single-cell data visualization (Figure 8); for this purpose, we selected 2 clusters: 299998, more abundant in EA patients, and 299996, more abundant in LA patients. Three markers (CD127, CD44, and CXCR3) whose expression was higher in the EA clusters are shown in Figure 8: 2 markers (CD45RA, CD38) that were more abundant in the LA clusters and 1 marker (PD-1) that did not show any expression difference between the clusters 299998 and 299996.

## Discussion

ART administration during the early phases of HIV-1 infection, possibly even during acute infection, may lead to a better preservation of immunological competence and reduced inflammation associated with long-term complications. The analyses of T cell phenotypes using flow cytometry in patients who began ART during the acute or chronic phase of infection showed that the frequencies of naive, CM, and EM CD4+ and CD8+ T cells in these patients were comparable (6); however, the results from the latter study were alarming (6), showing an equivalent expression of activation and differentiation molecules on T cells independent of the time of ART initiation. Pinpointing T cell biomarkers of successful ART initiated during early HIV-1 infection remains important to evaluate the preservation of immune competence in gen-
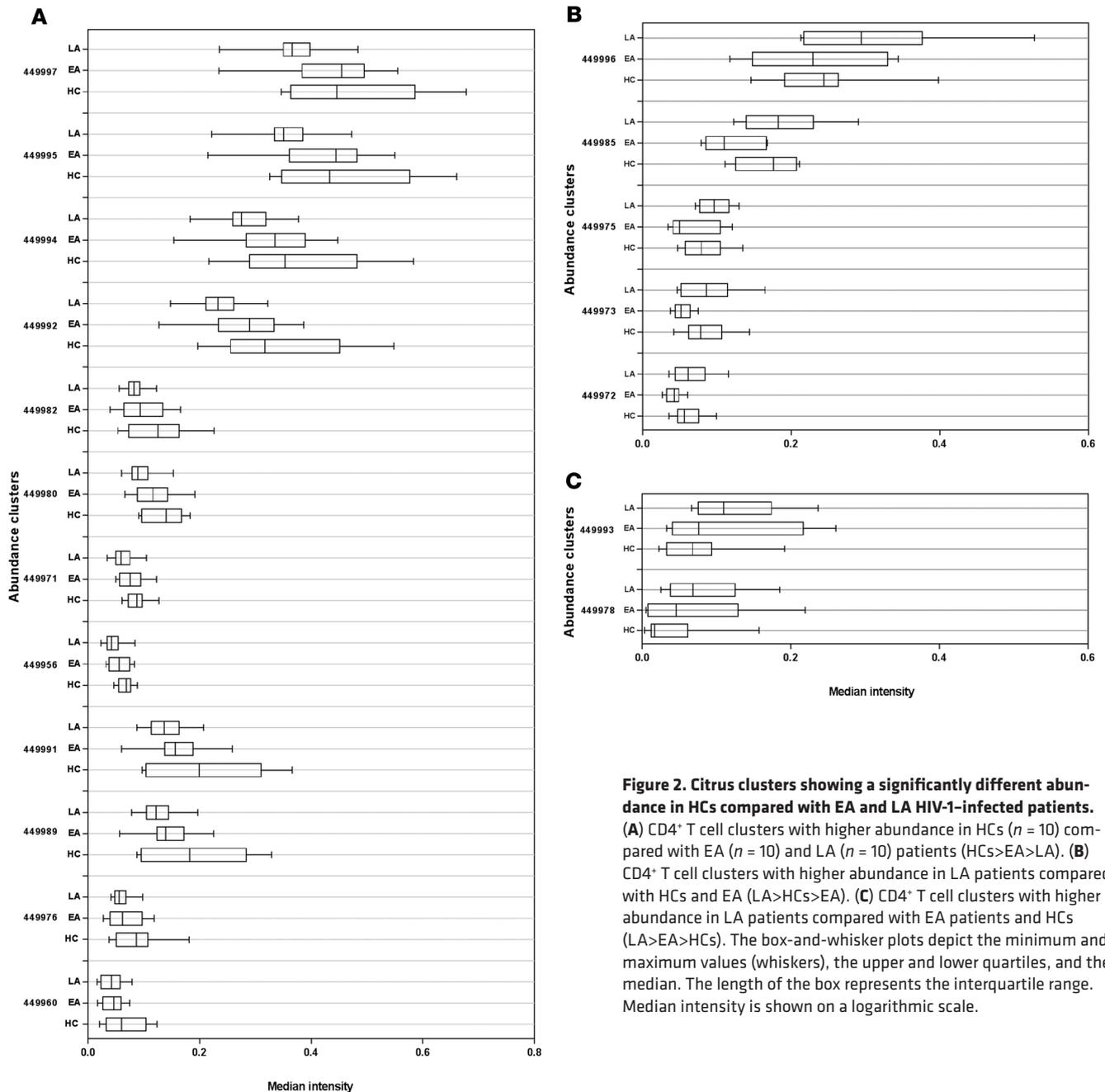
**Figure 2. Citrus clusters showing a significantly different abundance in HCs compared with EA and LA HIV-1–infected patients.**
(**A**) CD4+ T cell clusters with higher abundance in HCs (*n* = 10) compared with EA (*n* = 10) and LA (*n* = 10) patients (HCs>EA>LA). (**B**) CD4+ T cell clusters with higher abundance in LA patients compared with HCs and EA (LA>HCs>EA). (**C**) CD4+ T cell clusters with higher abundance in LA patients compared with EA patients and HCs (LA>EA>HCs). The box-and-whisker plots depict the minimum and maximum values (whiskers), the upper and lower quartiles, and the median. The length of the box represents the interquartile range. Median intensity is shown on a logarithmic scale.

eral and T cell function and phenotypes in particular. This will also be important to predict relevant post-treatment monitoring in patients interrupting ART for various reasons. In this context, the T cell exhaustion markers PD-1, Tim-3, and Lag-3, measured before ART initiation, were strong predictors of the time interval for reappearance of viremia upon ART interruption (20).

The application of mass cytometry to the study of T cell phenotypes during HIV-1 infection represents what we believe to be a new approach, allowing for the simultaneous evaluation of a large number of cell populations and many markers, with potential for better understanding of the complex changes occurring during HIV-1 infection. The features of exhausted CD8+ T cells were examined in several diseases, including HIV-1 infection, through an epigenomic-guided mass cytometry approach (21); the study, by creating a model of T cell exhaustion in humans, revealed that abnormally exhausted CD8+ T cell subpopulations were enriched in more advanced HIV disease. A recent study applied mass cytometry analysis to characterize the expression dynamics of CD32a on CD4+ T cells from HIV-1–infected patients during acute HIV-1 infection and ART (22); CD32a has been proposed to be a specific marker to identify latently HIV-infected CD4+ T cells. The results of the study
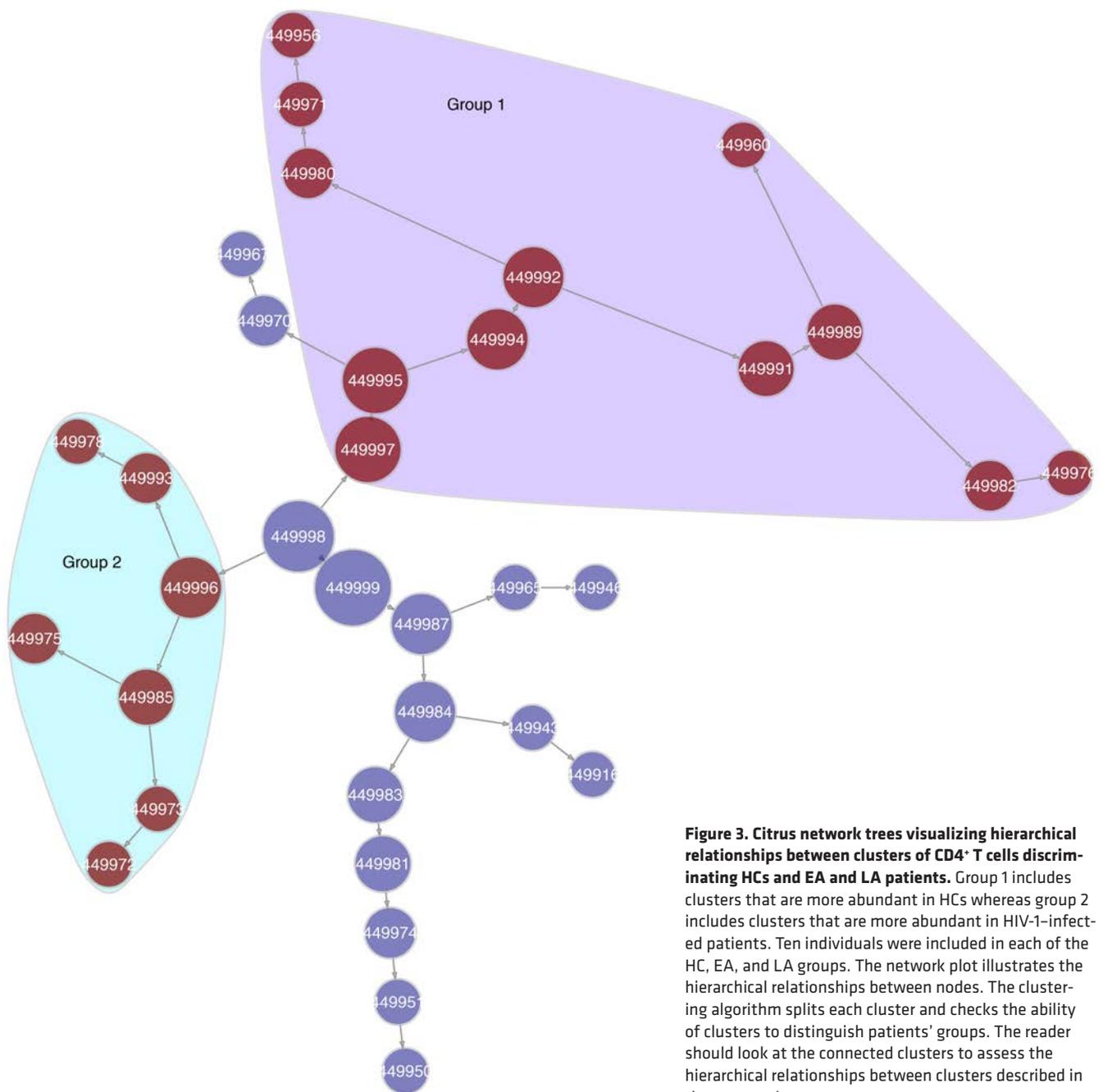
**Figure 3. Citrus network trees visualizing hierarchical relationships between clusters of CD4+ T cells discriminating HCs and EA and LA patients.** Group 1 includes clusters that are more abundant in HCs whereas group 2 includes clusters that are more abundant in HIV-1–infected patients. Ten individuals were included in each of the HC, EA, and LA groups. The network plot illustrates the hierarchical relationships between nodes. The clustering algorithm splits each cluster and checks the ability of clusters to distinguish patients' groups. The reader should look at the connected clusters to assess the hierarchical relationships between clusters described in the manuscript.

indicated that CD32a+ cells include heterogeneous CD4+ T cell subsets that are differentially affected during HIV-1 infection (22). The expression of CD127 (IL-7Rα), in a mass cytometry–based phenotyping study, identified a subset of memory CD4+ T cells that support HIV-1 entry but not viral gene expression (23).

In the present study, we aimed at assessing differences in T cell populations of HIV-1–infected patients who initiated ART during the acute or chronic phases of infection. Specific clusters distinguished CD4+ T cell populations of HCs and early- and late-treated patients; the high expression of CD44, CD127, CD28, and CD27 could be used to create a gradient of clusters that were more frequent in HCs compared with HIV-1–infected patients and in early ART–treated compared with late ART–treated patients.

The CD44 molecule is a receptor present on distinct T cell subpopulations that binds to HA (24) expressed in tissues. CD44 has been described to have multiple functions, and yet, it is incompletely characterized; CD44 has, however, a well-established role as an adhesion receptor important to position effector T cells at sites of inflammation and infection (25). Reduced levels of CD44 molecules
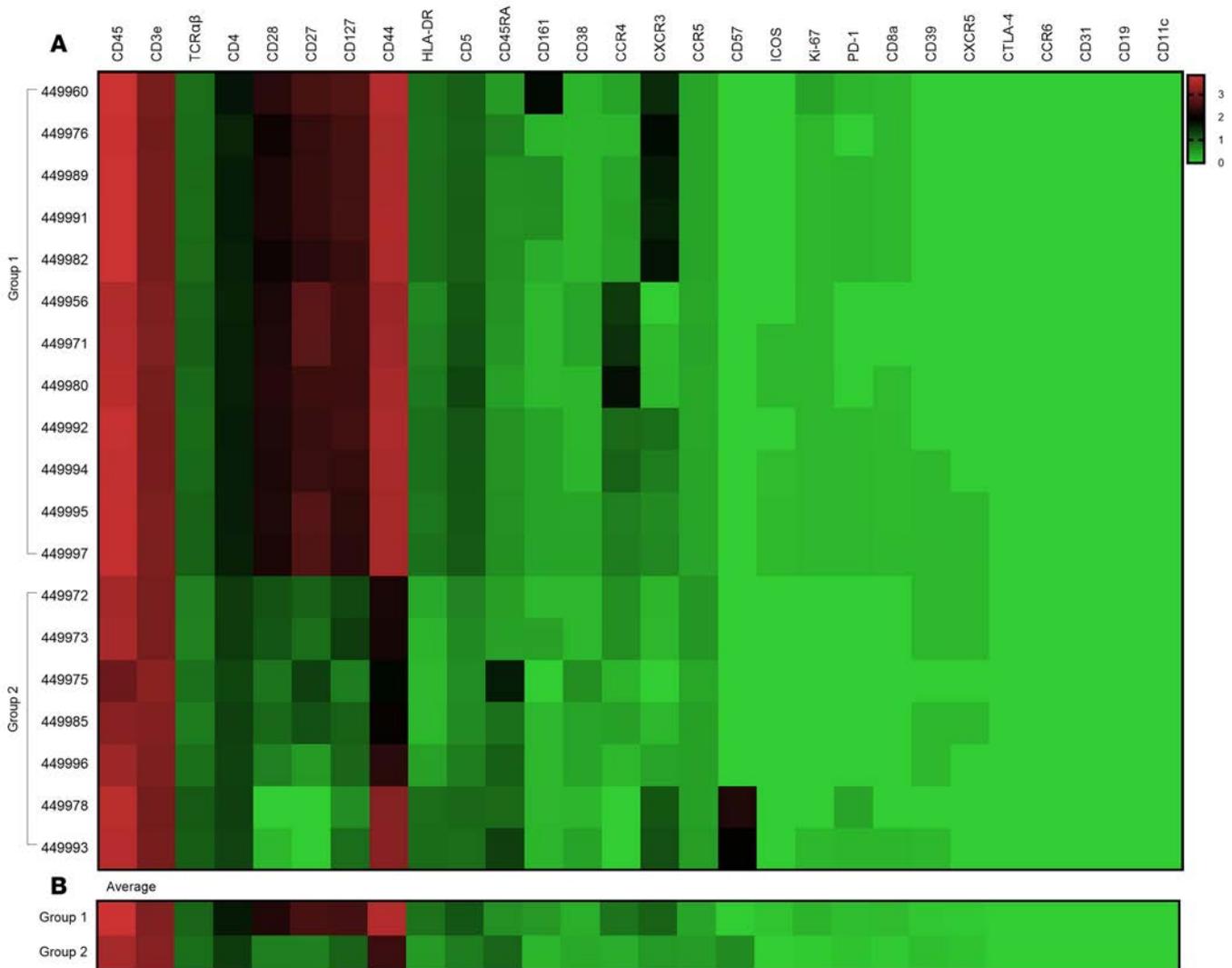
**Figure 4. Heatmaps visualizing the median metal intensity of individual markers in clusters that significantly distinguished HCs and EA and LA patients.** (**A**) The median metal marker intensity of individual clusters that were more abundant in HCs (group 1) and in EA and LA patients (group 2). (**B**) The average median metal intensity of groups 1 and 2. Ten individuals were included in each of the HC, EA, and LA groups.

during HIV-1 infection, especially in patients initiating treatment during the chronic phase of infection, may be involved in HIV-1 pathogenesis. In this context, CD44$^{lo}$ T cells may be impaired in their migration to inflamed tissues in response to upregulated HA expression produced by endothelial cells activated by inflammation products induced by virus replication (26). It is interesting to note that not only was CD44 expression on CD4$^+$ T cells reduced, but also CXCR3, a chemokine receptor involved in redirecting T cells to inflamed sites, declined. Whether reduced expression of CD44 and CXCR3 is a coordinated event of HIV-1 pathogenesis that is not corrected by ART initiated during the chronic phase of the disease needs to be addressed in further studies.

The role of CD44 as a mediator of T cell survival, especially of Th1 T cells, has also been reported; in this context, CD44 signaling via P13K/Akt may activate survival mechanisms in specialized T cell niches that contribute to memory T cell maintenance (27). Survival of memory T cells expressing CD44 has been postulated to occur by the orchestrated binding of IL-7 to its receptor (CD127) and HA to the CD44 receptor (28). It is interesting and noteworthy that in the present study, low expression of CD127 was detected in clusters with lower CD44 expression. A low expression of CD127 in CM and EM CD4$^+$ T cells was previously reported in both ART-naive and HIV-1 patients initiating treatment in the chronic phase of infection (29, 30), where low CD127 expression may limit the effect of IL-7 on T cell survival and homeostatic proliferation.

**Table 2. Average median metal intensity of markers distinguishing clusters that were more abundant in HCs (group 1), HIV-1–infected patients (group 2), EA patients (group 3), or LA (group 4) patients**

|  | CD45 | CD3-ε | TCR-αβ | CD4 | CD28 | CD27 | CD127 | CD44 | HLA-DR | CD5 | CD45RA | CD161 | CD38 | CCR4 |
|---|---|---|---|---|---|---|---|---|---|---|---|---|---|---|
| Group 1 | 3.74 | 3.04 | 0.95 | 1.64 | 2.18 | 2.52 | 2.48 | 3.5 | 0.83 | 1.1 | 0.55 | 0.47 | 0.27 | 0.81 |
| Group 2 | 3.38 | 3.08 | 0.86 | 1.33 | 0.7 | 0.69 | 0.97 | 2.39 | 0.45 | 0.73 | 0.95 | 0.2 | 0.33 | 0.28 |
| Group 3 | 3.57 | 3.13 | 1.05 | 1.69 | 2.22 | 2.64 | 2.3 | 3.47 | 0.77 | 1.13 | 0.53 | 0.34 | 0.38 | 0.85 |
| Group 4 | 3.21 | 3.25 | 0.97 | 1.43 | 1.3 | 1.82 | 1.24 | 2.33 | 0.24 | 0.73 | 1.48 | 0.19 | 0.63 | 0.3 |

Another functional characteristic of the CD44 receptor creates an additional link with the results presented here. CD44 signaling has been shown to interfere with Fas-mediated apoptosis, a mechanism that CD44 shares with the CD28 costimulatory molecule (28). The T cell clusters that we found to be more abundant in HIV-1–infected patients, especially in the late-treated patients, displayed a lower expression of both CD44 and CD28 molecules. According to our findings, the expression of 3 molecules (CD44, CD28, and CD127), all important for mediating T cell survival, is reduced in T cells of HIV-1–infected patients, especially in patients receiving treatment during the chronic phase of infection. Fas-mediated apoptosis has been shown in multiple studies to be linked to T cell apoptosis occurring during HIV-1 infection (31). T cells of patients treated late during infection may, accordingly, have a reduced survival upon reduced uptake of IL-7 and activation of Fas-mediated apoptosis because of a reduced expression of CD44 and CD28.

In patients receiving ART, the expression of CD27 and CD28 on *ex vivo* CD4^{+} T cells was lower in patients with low CD4^{+} T cell counts compared with patients with normal CD4^{+} T cell counts (32); the frequency of CD4^{+} T cells expressing CD27 and CD28 inversely correlated with CD4^{+} T cell expression of activation and senescence markers, including Fas. In addition, poor proliferative responses of CD4^{+} T cells were linked to impaired induction of CD27 and CD28 on CD4^{+} T cells activated in vitro (32).

Previous studies have assessed CD44 expression on T cells during HIV-1 infection. To characterize homing dysfunctions of CD4^{+} and CD8^{+} T cells in HIV-1–infected patients, CD44 expression on blood cells was studied in parallel to other adhesion molecules (33). CD44 expression was reduced on both CD4^{+} and CD8^{+} T cells in HIV-1–infected patients with CD4^{+} T cell counts less than 200 and AIDS-defining conditions; the decline was less evident in patients presenting with CD4^{+} T cells greater than 200 (33). CD44 has been studied to clarify whether this molecule has an impact on HIV-1 infection (34), and the results indicated that in human leukocytes, the standard hematopoietic form of CD44 (defined as CD44S) is an important determinant of HIV-1 productive infection and, possibly, of HIV-1 cellular tropism. Very few studies have addressed whether CD44 expression on T cells changes in HIV-1 patients initiating ART. Turnover of CD4^{+} T cells during the first weeks following ART initiation occurs mostly in memory cells, which recirculate through lymphoid organs (CD62L^{+} and CD44^{lo}), whereas memory T cells with the homing phenotype of CD4^{+} T cells (CD62L^{−} and CD44^{hi}) recirculating from blood to tissue appear to have a minor role in turnover (35). In a recent study (36) aimed at evaluating fluctuations of endothelial function and proatherosclerotic biomarkers in HIV-1–infected patients initiating 2 different protease inhibitor–based regimens, it was shown that the frequency of CD4^{+} T cells expressing the adhesion molecule CD44 increased significantly during both treatment regimens.

**Table 3. Average median metal intensity of markers distinguishing clusters that were more abundant in HCs (group 1), HIV-1–infected patients (group 2), EA patients (group 3), or LA (group 4) patients**

|  | CXCR3 | CCR5 | CD57 | ICOS | Ki-67 | PD-1 | CD8a | CD39 | CXCR5 | CTLA-4 | CCR6 | CD31 | CD19 | CD11c |
|---|---|---|---|---|---|---|---|---|---|---|---|---|---|---|
| Group 1 | 0.97 | 0.37 | 0 | 0.07 | 0.21 | 0.13 | 0.15 | 0.05 | 0.03 | 0 | 0 | 0 | 0 | 0 |
| Group 2 | 0.47 | 0.43 | 0.59 | 0 | 0.03 | 0.08 | 0.03 | 0.13 | 0.08 | 0 | 0 | 0 | 0 | 0 |
| Group 3 | 0.55 | 0.37 | 0 | 0.14 | 0.19 | 0.16 | 0.18 | 0.12 | 0.52 | 0 | 0 | 0 | 0 | 0 |
| Group 4 | 0.08 | 0.42 | 0 | 0 | 0 | 0 | 0 | 0.15 | 0.08 | 0 | 0 | 0 | 0 | 0 |
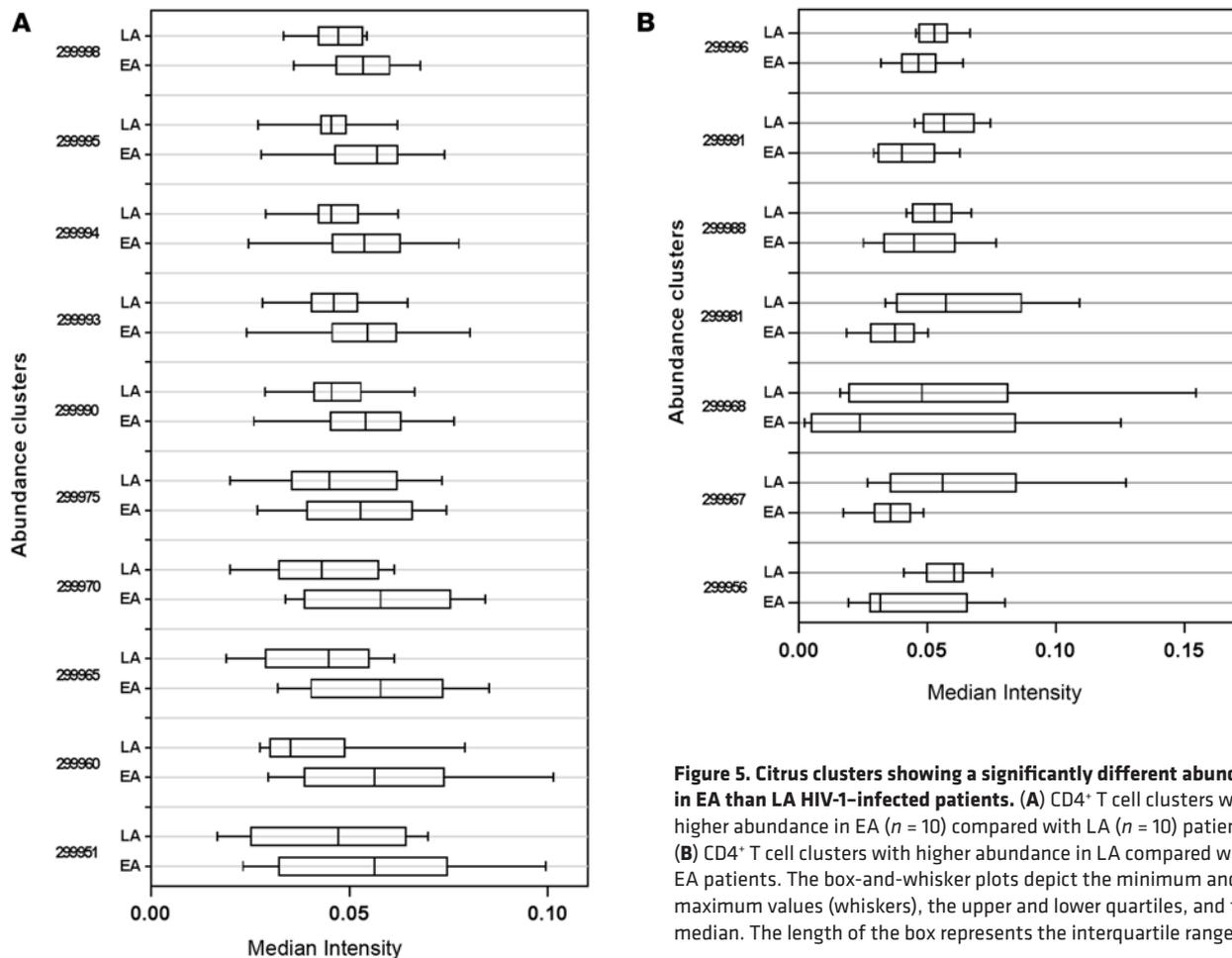
**Figure 5. Citrus clusters showing a significantly different abundance in EA than LA HIV-1–infected patients.** (**A**) CD4+ T cell clusters with higher abundance in EA (*n* = 10) compared with LA (*n* = 10) patients. (**B**) CD4+ T cell clusters with higher abundance in LA compared with EA patients. The box-and-whisker plots depict the minimum and maximum values (whiskers), the upper and lower quartiles, and the median. The length of the box represents the interquartile range.

Our study is the first to our knowledge to show the presence of specific T cell population changes associated with the time of ART initiation during acute and chronic HIV-1 infection, respectively. Our observation of a gradient signature involving CD44, CD27, CD127, and CD28 expression on CD4+ T cell clusters, which were more abundant in HCs and early-treated and late-treated HIV-1–infected patients, respectively, suggests that ART initiated during chronic HIV-1 infection may not correct for signatures of impaired T cell survival and senescence during HIV-1 infection. Early ART improves this phenomenon and the expression of CD44, CD27, CD127, and CD28 in clusters that were more abundant in early-treated patients was similar to what was found in the clusters abundant in HCs. Further studies need to assess whether CD44 expression, possibly combined with CD127, CD27, and CD28, may be a useful biomarker to predict the ability to control HIV-1 in patients on long-term ART (4).

## Methods

*Study participants.* Twenty HIV-1–infected individuals and 10 age-matched HCs were recruited at the Department of Infectious Diseases, Södersjukhuset, Stockholm. HIV-1–infected participants were grouped according to the time of ART initiation; the EA group received ART within 9 days of a positive p24 antigen test (Fiebig stage II), except 1 patient who started ART 28 days after a positive HIV-1 serology chemiluminescent microparticle immunoassay (Fiebig stage V). This patient had a negative p24 antigen test 1 month before. The LA group initiated treatment during the chronic phase of HIV-1 infection.

At the time of sampling, EA and LA patients had been on ART for a mean of 26 and 31 months, respectively; RNA copies per milliliter were below the detection limits (<20 copies/ml) in both groups. The clinical parameters of the patients, including the length of ART treatments and the number of HIV-1 DNA copies in PBMCs, are shown in Table 1. The patients and HCs included in the study were part of a previous study (6) assessing parameters of immune activation and exhaustion of T cells by
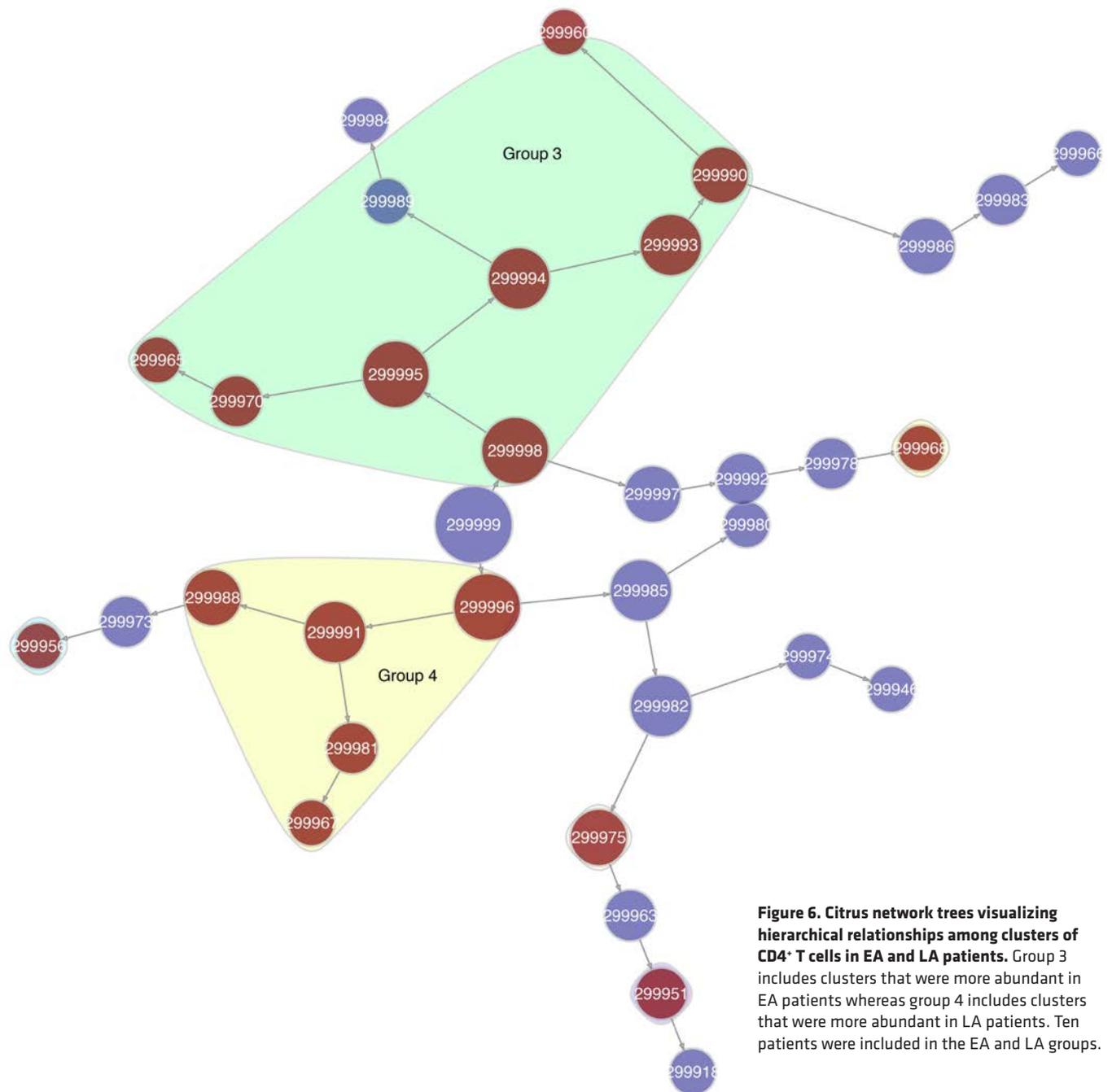
**Figure 6. Citrus network trees visualizing hierarchical relationships among clusters of CD4+ T cells in EA and LA patients.** Group 3 includes clusters that were more abundant in EA patients whereas group 4 includes clusters that were more abundant in LA patients. Ten patients were included in the EA and LA groups.

flow cytometry according to the time of ART initiation.

Blood (30 ml) was collected aseptically from patients and controls in EDTA-containing tubes; PBMCs were isolated and stored in 90% FBS and 10% DMSO (Sigma-Aldrich) in liquid nitrogen (–196°C) until further analyses were conducted.

*Immunostainings of T cell subpopulations.* Isolated PBMCs were stained using fluorochrome-conjugated antibodies in different combinations: anti–CD3-ε (UCHT1), anti-CD4 (Clone L200), anti-CD8 (SK1), anti-CD45RA (HI100), and anti-CCR7 (3D12), all from BD Biosciences. A LIVE/DEAD Fixable Near-IR kit (Life Technologies Europe BV) was used to exclude dead cells from the analyses. Stained cells were washed 3 times with PBS before being fixed in 2% paraformaldehyde. All antibodies were used at the concentrations determined after titration experiments. Matched isotype controls or fluorescence minus 1 were used to set the gating strategies. Fluorescence intensities were measured with LSRII (BD Biosciences), and data were analyzed using FlowJo, version 9.4.11 (Tree Star Inc).
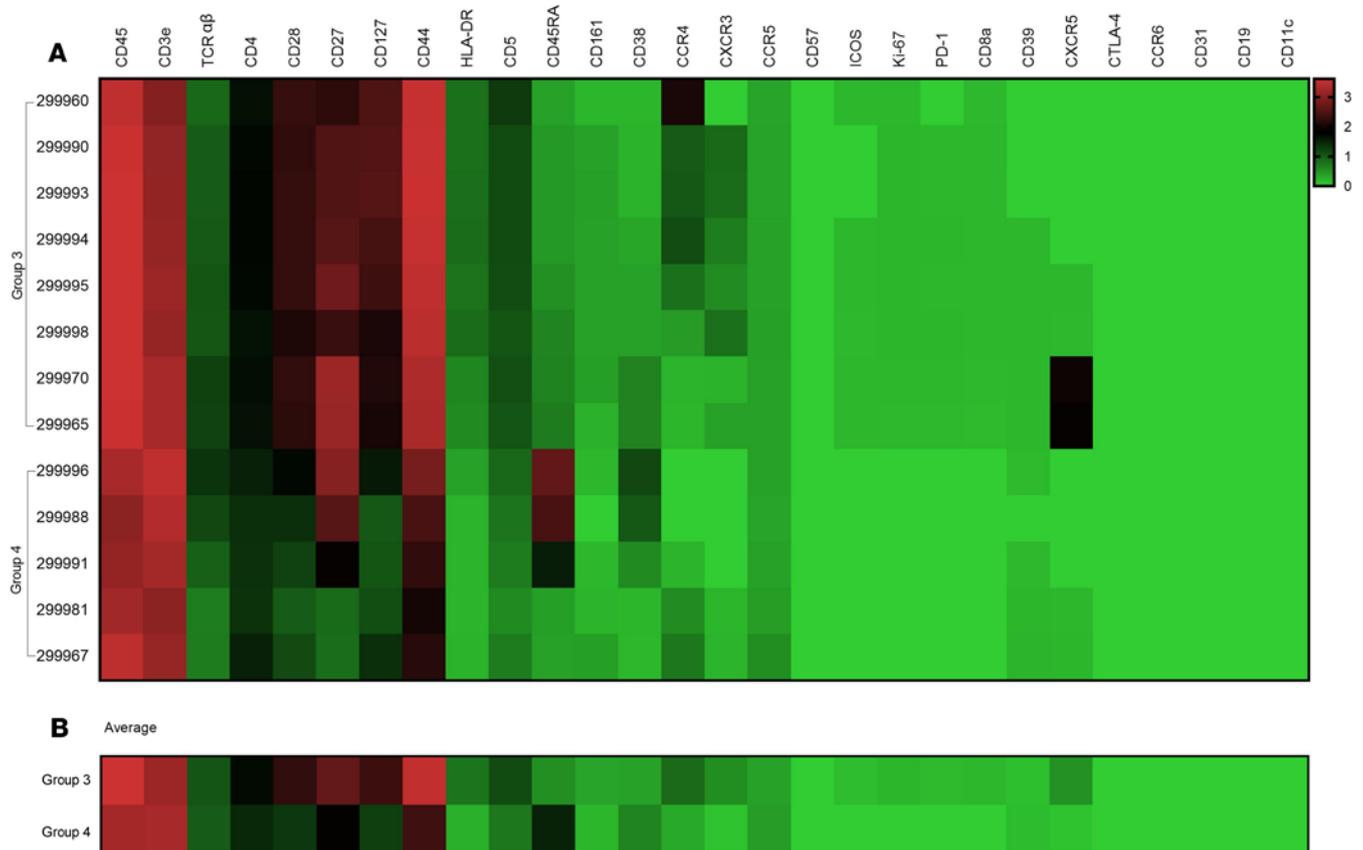
**Figure 7. Heatmaps visualizing the intensity of individual markers in clusters that significantly distinguished EA and LA patients.** (**A**) The marker intensity of individual clusters that were more abundant in EA patients (group 3) and in LA patients (group 4). (**B**) The average median metal intensity of groups 3 and 4. Ten patients were included in each of the EA and LA groups.

T cell subsets were gated out using the following antibody combinations: naive CD4$^+$ (CD3$^+$CD4$^+$CD8$^-$CD45RA$^+$CCR7$^+$), EM CD4$^+$ (CD3$^+$CD4$^+$CD8$^-$CD45RA$^-$CCR7$^-$), and CM CD4$^+$ (CD3$^+$CD4$^+$CD8$^-$CD45RA$^-$CCR7$^+$).

*Mass cytometry*. Before mass cytometry analysis, PBMCs were thawed in RPMI medium supplemented with 10% FBS, 1% penicillin-streptomycin, and 25 U/ml benzonase (Sigma-Aldrich) and rested overnight in a $CO_2$ incubator at 37°C.

For live–dead cell distinction, cells were stained with 2.5 µM cisplatin (Fluidigm) in RPMI without serum for 5 minutes at room temperature and quenched with RPMI containing FBS. An Agilent robotic platform was used for staining cells because this offers a more uniform staining and less variability among samples. Cells were then resuspended in CyFACS buffer (PBS with 0.1% BSA, 0.05% sodium azide, and 2 µM EDTA) and counted; approximately 2 million live cells were used for staining in a 96-well, round-bottom plate. Next, cells were incubated for 30 minutes at 4°C with a 30-µl cocktail of metal-conjugated antibodies targeting surface antigens in a T cell panel (Supplemental Table 1; supplemental material available online with this article; https://doi.org/10.1172/jci.insight.125442DS1). Following washes with CyFACS buffer and overnight fixation using 1% formaldehyde made in PBS (Polysciences Inc), cells were permeabilized using an intracellular fixation and permeabilization buffer set (eBiosciences Inc) according to the manufacturer's recommendations and stained with 30 µl of intracellular antibody cocktail (Ki-67) for 60 minutes at room temperature. Cells were washed and fixed in 1% formaldehyde at 4°C.

Before acquisition, staining was conducted for 20 minutes at room temperature with a 191/193Ir DNA intercalator (Fluidigm), which binds to nucleic acids for event recognition during acquisition. After washing with PBS and Milli-Q water (MilliporeSigma), cells were acquired by a CyTOF 2 mass cytometer (Fluidigm) at a rate of 300–500 cells/second with noise reduction, a lower convolution threshold of 200, event length limits of 10–15 pushes, a sigma value of 3, and a flow rate of 0.045 ml/minute.
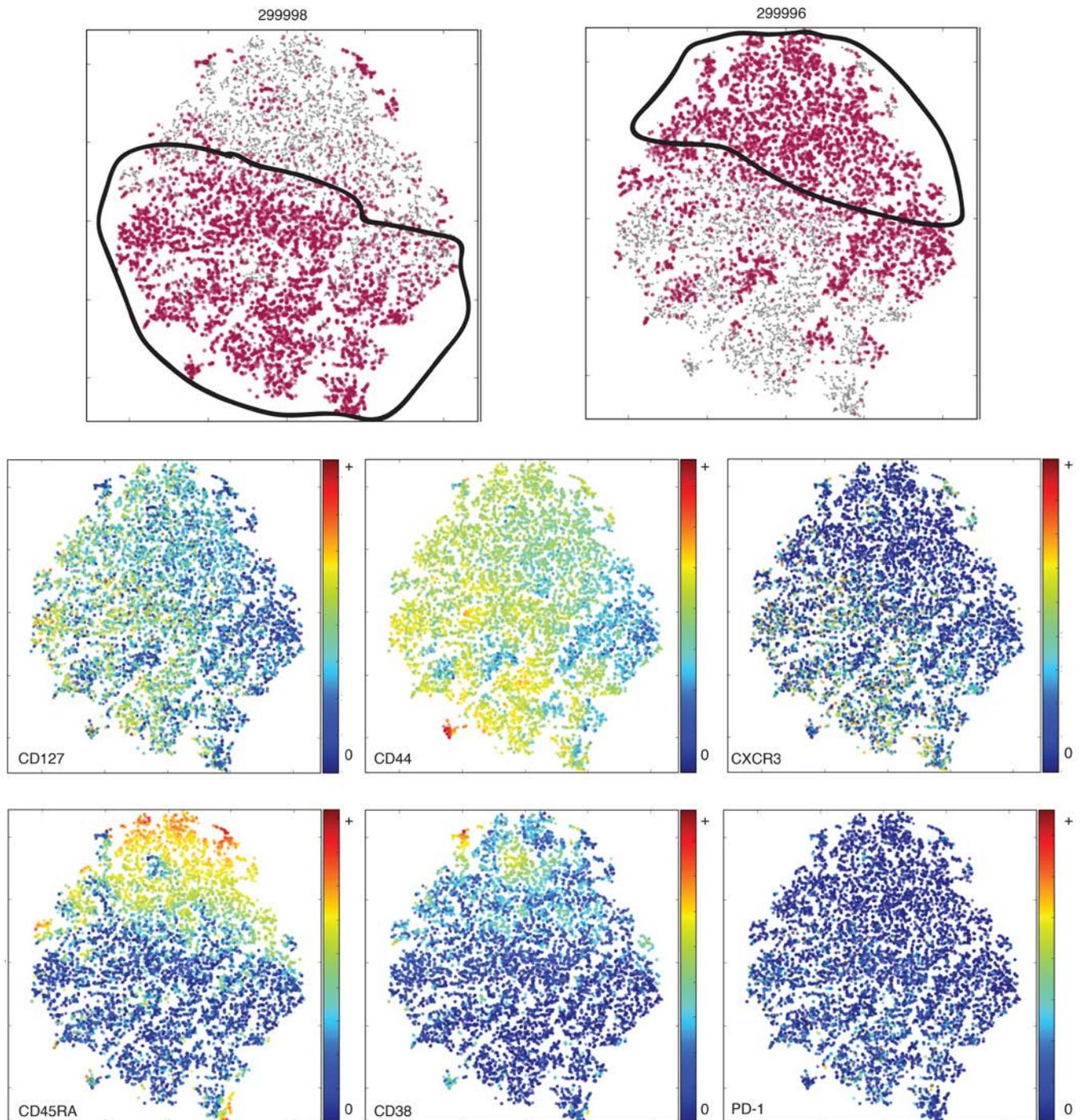
**Figure 8. Phenotypic differences of clusters that were more abundant in EA or LA patients illustrated by t-SNE single-cell data visualization.** The t-SNE plots show 3 markers (CD127, CD44, and CXCR3) whose median metal intensity was higher in the EA cluster (cluster 299998), 2 markers (CD45A and CD38) that were more abundant in the LA cluster (cluster 299996), and 1 marker (PD-1) that did not show any intensity difference between the 299998 and 299996 clusters. Ten patients were included in each of the EA and LA groups.

The mass cytometry analysis was conducted on the 30 specimens 1 time.

*Data analysis*. Data were analyzed by the identification of cell events (DNA$^{hi}$) and exclusion of dead or dying cells (cisplatin$^{+}$). Live cells were analyzed for 28 phenotypic markers. The Citrus algorithm was used to identify, in an unbiased fashion, differently abundant cell populations in HIV-1–infected groups and HCs (14).

Heatmaps were generated to visualize average marker expression in the clusters of cells identified by Citrus. Dimensionality reduction of unclustered data was conducted using the t-SNE algorithm that is imple-

mented in the Cytofkit library (11), supplied by Bioconductor version 3.4 (37), and run in RStudio version 1.0.44. A fixed number of 5,000 cells was sampled without replacement from each file and combined for analysis. The following markers were used for clustering: CD45, CD57, CCR6, CD5, CCR5, CD4, CD8a, CD31, ICOS, TCR-αβ, CD3-ε, CCR4, CXCR3, CD28, CD161, Ki-67, HLA-DR, CD44, CD127, CD27, CD38, CD45RA, CTLA-4, PD-1, CD39, CXCR5, CD19, and CD11c. The resulting t-SNE plots were then filtered by marker expression and EA and LA patient groups to visualize differences between both the patient groups.

*Statistics*. To compare the frequencies of T cell subpopulations between groups of patients and controls (Figure 1), ANOVA was applied. The differences in clinical and immunological parameters (Table 1) were assessed by a 2-tailed *t* test; a *P* value < 0.05 was considered significant.

*Study approval*. The ethical committee at Karolinska Institutet (Stockholm, Sweden) reviewed and approved the study. All patients provided written informed consent before their participation in the study.

## Author contributions

YB conducted experiments, analyzed the data, created figures, and wrote the manuscript. TL conducted experiments, analyzed the data, and created figures. YC analyzed the data and created figures. JM conducted experiments, analyzed the data, and created figures. AN analyzed the data, created figures, and wrote part of the manuscript. SP analyzed the data and created figures. BH selected the individuals to be recruited to the study, analyzed the clinical characteristics, and wrote parts of the manuscript. PB planned the study, analyzed the data, and wrote the manuscript. FC planned the study, analyzed the data, and wrote the manuscript.

## Acknowledgments

Address correspondence to: Francesca Chiodi, Department of Microbiology, Tumor and Cell Biology, Biomedicum, Karolinska Institutet, Solnavägen 9, 17165 Solna, Sweden. Phone: 46.8.52486315; Email: francesca.chiodi@ki.se.

1. INSIGHT START Study Group, et al. Initiation of antiretroviral therapy in early asymptomatic HIV infection. *N Engl J Med*. 2015;373(9):795–807.

2. SPARTAC Trial Investigators, et al. Short-course antiretroviral therapy in primary HIV infection. *N Engl J Med*. 2013;368(3):207–217.

3. Barton K, Winckelmann A, Palmer S. HIV-1 Reservoirs during suppressive therapy. *Trends Microbiol*. 2016;24(5):345–355.

4. Sáez-Cirión A, et al. Post-treatment HIV-1 controllers with a long-term virological remission after the interruption of early initiated antiretroviral therapy ANRS VISCONTI Study. *PLoS Pathog*. 2013;9(3):e1003211.

5. Hey-Cunningham WJ, et al. Early antiretroviral therapy with raltegravir generates sustained reductions in HIV reservoirs but not lower T-cell activation levels. *AIDS*. 2015;29(8):911–919.

6. Amu S, et al. Dysfunctional phenotypes of CD4+ and CD8+ T cells are comparable in patients initiating ART during early or chronic HIV-1 infection. *Medicine (Baltimore)*. 2016;95(23):e3738.

7. Brenchley JM, et al. CD4+ T cell depletion during all stages of HIV disease occurs predominantly in the gastrointestinal tract. *J Exp Med*. 2004;200(6):749–759.

8. Deleage C, et al. Impact of early cART in the gut during acute HIV infection. *JCI Insight*. 2016;1(10):e87065.

9. Brodin P, et al. Variation in the human immune system is largely driven by non-heritable influences. *Cell*. 2015;160(1–2):37–47.

10. Mason GM, et al. Phenotypic complexity of the human regulatory T cell compartment revealed by mass cytometry. *J Immunol*. 2015;195(5):2030–2037.

11. Wong MT, et al. Mapping the diversity of follicular helper T cells in human blood and tonsils using high-dimensional mass cytometry analysis. *Cell Rep*. 2015;11(11):1822–1833.

12. Lau AH, et al. Mass cytometry reveals a distinct immunoprofile of operational tolerance in pediatric liver transplantation. *Pediatr Transplant*. 2016;20(8):1072–1080.

13. Kaczorowski KJ, et al. Continuous immunotypes describe human immune variation and predict diverse responses. *Proc Natl Acad Sci U S A*. 2017;114(30):E6097–E6106.

14. Bruggner RV, Bodenmiller B, Dill DL, Tibshirani RJ, Nolan GP. Automated identification of stratifying signatures in cellular subpopulations. *Proc Natl Acad Sci U S A*. 2014;111(26):E2770–E2777.

15. Shekhar K, Brodin P, Davis MM, Chakraborty AK. Automatic classification of cellular expression by nonlinear stochastic embedding (ACCENSE). *Proc Natl Acad Sci U S A*. 2014;111(1):202–207.

16. Van der Maaten LJP, Hinton GE. Visualizing high-dimensional data using t-SNE. *J Mach Learn Res*. 2008;9:2579–2605.

17. Schumann J, Stanko K, Schliesser U, Appelt C, Sawitzki B. Differences in CD44 surface expression levels and function discriminates IL-17 and IFN-γ producing Helper T cells. *PLoS One*. 2015;10(7):e0132479.

18. Brenchley JM, et al. Expression of CD57 defines replicative senescence and antigen-induced apoptotic death of CD8+ T cells. *Blood*. 2003;101(7):2711–2720.

19. Palmer BE, Blyveis N, Fontenot AP, Wilson CC. Functional and phenotypic characterization of CD57+CD4+ T cells and their association with HIV-1-induced T cell dysfunction. *J Immunol*. 2005;175(12):8415–8423.

20. Hurst J, et al. Immunological biomarkers predict HIV-1 viral rebound after treatment interruption. *Nat Commun*. 2015;6:8495.

21. Bengsch B, et al. Epigenomic-guided mass cytometry profiling reveals disease-specific features of exhausted CD8 T cells. *Immunity*. 2018;48(5):1029–1045.e5.

22. Coindre S, et al. Mass cytometry analysis reveals the landscape and dynamics of CD32a+ CD4+ T cells from early HIV infection to effective cART. *Front Immunol*. 2018;9:1217.

23. Cavrois M, et al. Mass cytometric analysis of HIV entry, replication, and remodeling in tissue CD4+ T cells. *Cell Rep*. 2017;20(4):984–998.

24. Baaten BJ, Li CR, Bradley LM. Multifaceted regulation of T cells by CD44. *Commun Integr Biol*. 2010;3(6):508–512.

25. DeGrendele HC, Estess P, Siegelman MH. Requirement for CD44 in activated T cell extravasation into an inflammatory site. *Science*. 1997;278(5338):672–675.

26. Ley K, Laudanna C, Cybulsky MI, Nourshargh S. Getting to the site of inflammation: the leukocyte adhesion cascade updated. *Nat Rev Immunol*. 2007;7(9):678–689.

27. Baaten BJ, Li CR, Deiro MF, Lin MM, Linton PJ, Bradley LM. CD44 regulates survival and memory development in Th1 cells. *Immunity*. 2010;32(1):104–115.

28. Baaten BJ, Tinoco R, Chen AT, Bradley LM. Regulation of antigen-experienced T cells: lessons from the quintessential memory marker CD44. *Front Immunol*. 2012;3:23.

29. Rethi B, et al. Loss of IL-7Rα is associated with CD4 T-cell depletion, high interleukin-7 levels and CD28 down-regulation in HIV infected patients. *AIDS*. 2005;19(18):2077–2086.

30. Potter SJ, et al. Preserved central memory and activated effector memory CD4+ T-cell subsets in human immunodeficiency virus controllers: an ANRS EP36 study. *J Virol*. 2007;81(24):13904–13915.

31. Gougeon ML. Apoptosis as an HIV strategy to escape immune attack. *Nat Rev Immunol*. 2003;3(5):392–404.

32. Tanaskovic S, Price P, French MA, Fernandez S. Impaired upregulation of the costimulatory molecules, CD27 and CD28, on CD4+ T cells from HIV patients receiving ART is associated with poor proliferative responses. *AIDS Res Hum Retroviruses*. 2017;33(2):101–109.

33. Hayes PJ, Miao YM, Gotch FM, Gazzard BG. Alterations in blood leucocyte adhesion molecule profiles in HIV-1 infection. *Clin Exp Immunol*. 1999;117(2):331–334.

34. Dukes CS, et al. Cellular CD44S as a determinant of human immunodeficiency virus type 1 infection and cellular tropism. *J Virol*. 1995;69(7):4000–4005.

35. Hengel RL, Jones BM, Kennedy MS, Hubbard MR, McDougal JS. Markers of lymphocyte homing distinguish CD4 T cell subsets that turn over in response to HIV-1 infection in humans. *J Immunol*. 1999;163(6):3539–3548.

36. Squillace N, et al. Evaluation of adhesion molecules and immune parameters in HIV-infected patients treated with an atazanavir/ritonavir- compared with a lopinavir/ritonavir-based regimen. *J Antimicrob Chemother*. 2018;73(8):2162–2170.

37. Gentleman RC, et al. Bioconductor: open software development for computational biology and bioinformatics. *Genome Biol*. 2004;5(10):R80.